Inorg. Chem. **2003**, *42*, 5545–5550

Products of the Electrochemical Oxidation of *cis*-$L_2Ru^{(II)}(NCS)_2$ in Dimethylformamide and Acetonitrile Determined by LC-UV/Vis-MS

Gregers Hansen, Bo Gervang, and Torben Lund*

Department of Life Sciences and Chemistry, Roskilde University, DK-4000, Denmark

Received December 26, 2002

The bis tetrabutylammonium salt of the solar cell dye, $L_2Ru(NCS)_2$, $((Bu_4N^+)_2\,[Ru(dcbpyH)_2(NCS)_2]^{2-})$, was oxidized electrochemically in both dimethylformamide and acetonitrile. Four different ruthenium complexes were identified by LC-UV/Vis-MS during the electrochemical oxidation process in dimethylformamide. The formation of the four complexes may be explained by a competition between a solvent-independent route with the formation of the intermediate complex $L_2Ru(NCS)(CN)$ and the final oxidation product $L_2Ru(CN)_2$ and a solvent-dependent route, which proceeds through the intermediate complex $L_2Ru(NCS)(DMF)^+$ to the final product $L_2Ru(CN)(DMF)^+$. In acetonitrile the solvent-dependent mechanism is dominant and only the oxidation products $L_2Ru(NCS)(ACN)^+$ and $L_2Ru(CN)(ACN)^+$ were identified.

Introduction

The ruthenium complex *cis*-$L_2Ru^{(II)}(NCS)_2$ (L = dcbpyH$_2$ = 2,2′-bipyridine-4,4′-dicarboxylic acid) has been shown by Grätzel and co-workers to be a very efficient and stable sensitizer for the dye-sensitized nanocrystalline TiO_2 solar cell (Figure 1).[1−3]

The chemistry at the photo anode is shown in eqs 1−3:

$$TiO_2|L_2Ru^{(II)}(NCS)_2 + h\nu \rightarrow TiO_2|L_2Ru^{(II)}(NCS)_2^* \quad (1)$$

$$TiO_2|L_2Ru^{(II)}(NCS)_2^* \rightarrow TiO_2 + e^-|L_2Ru^{(III)}(NCS)_2^+ \quad (2)$$

$$TiO_2|L_2Ru^{(III)}(NCS)_2^+ + I^- \rightarrow TiO_2|L_2Ru^{(II)}(NCS)_2 + I^\bullet \quad (3)$$

The ruthenium dye, which is anchored to the TiO_2 surface by an ester bond, is excited by the incoming light and transformed to the oxidized form by an ultrafast electron injection process from the excited state to the conduction band of the TiO_2 semiconductor. The chemistry of the photo anode is completed by the regeneration of the starting complex by an electron transfer from the mediator I^-.[1,2]

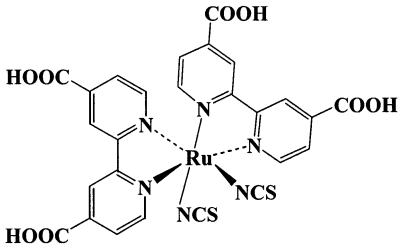

Figure 1. $L_2Ru^{(II)}(NCS)_2$.

The *cis*-$L_2Ru^{(II)}(NCS)_2$ complex has been shown to be very stable.[4] However, the compound is unstable in its oxidized state, which is apparent from the irreversible voltammograms of the complex.[5,6] The stability of the dye during solar cell operation is therefore dependent on the rate of regeneration of the $Ru^{(II)}$ dye compared with the rate of degradation of the $Ru^{(III)}$ complex. Knowledge of the oxidation products of $L_2Ru^{(II)}(NCS)_2$ and the rate of the degradation is therefore essential for the prediction of the long-term stability of the solar cell.

Wolfbauer et al. have studied the electrochemical oxidation of the diethylester of $L_2Ru^{(II)}(NCS)_2$ in both dimethylformamide and acetonitrile and have proposed the following

* Author to whom correspondence should be addressed. Fax: 45-46743011. E-mail: tlund@ruc.dk.

(1) Hagfeldt, A.; Grätzel, M. *Acc. Chem. Res.* **2000**, *33*, 269.
(2) Grätzel, M. *Nature* **2001**, *414*, 338.
(3) Nazeeruddin, M. K.; Kay, A.; Rodicio, I.; Humphry-Baker, R.; Muller, E.; Liska, P.; Vlachopoulos, N.; Grätzel, M. *J. Am Chem. Soc.* **1993**, *1993*, 6382.
(4) Amirnasr, M.; Nazeeruddin, Md. K.; Grätzel, M. *Thermochim. Acta* **2000**, *348*, 105.
(5) Bond, A. M.; Deacon, G. B.; Howitt, J.; MacFarlane, D. R.; Spiccia, L.; Wolfbauer, G. *J. Electrochem. Soc.* **1999**, *146* (7), 648.
(6) Wolfbauer, G.; Bond, A. M.; MacFarlane, D. R. *Inorg. Chem.* **1999**, *38*, 3836.

10.1021/ic0207294 CCC: $25.00
Published on Web 08/06/2003

oxidation scheme eqs 4 and 5:[6]

$$L_2Ru^{(II)}(NCS)_2 \rightarrow L_2Ru^{(III)}(NCS)_2^{+} + e^{-} \quad (4)$$

$$L_2Ru^{(III)}(NCS)_2^{+} \rightarrow L_2Ru^{(II)}(CN)_2 + 5e^{-} + \text{oxidized "S"} \quad (5)$$

The oxidation was found to proceed directly to the dicyanide complex $L_2Ru^{(II)}(CN)_2$ by a total liberation of 6 ± 2 electrons.[6] The initial step of eq 5 is likely to proceed via an internal electron transfer between the NCS^- ligand and the $Ru^{(III)}$ central atom. The dicyanide complex may also be obtained by photolysis of $L_2Ru(NCS)_2$ in methanol and by oxidation of $L_2Ru(NCS)_2$ with D_2O_2 in aqueous solution.[7] In contrast to the results of Wolfbauer, Kohle et al.[7] were able to show by in situ NMR spectroscopy that the dicyano complex was formed via an intermediate mixed thiocyanate−cyanide complex $L_2Ru^{(II)}(NCS)(CN)$.[7] Very recently, the electrochemical oxidation of $L_2Ru(NCS)_2$ was investigated in acetonitrile (ACN) by cyclic voltammetry, UV and infusion electrospray mass spectrometry (ESI-MS) and a solvent dependent oxidation mechanism was proposed, which involved the complex $L_2Ru^{(II)}(NCS)(ACN)^+$ and the end oxidation product $L_2Ru^{(II)}(ACN)_2^{2+}$.[8]

As evident from the above brief literature summary, a clear picture of the intermediate products and mechanism of the $L_2Ru(NCS)_2$ oxidation is still not established. We therefore decided to perform a reinvestigation of the electrochemical oxidation process of $L_2Ru^{(II)}(NCS)_2$ in dimethylformamide and acetonitrile by HPLC coupled to a photodiode array and an ion trap mass detector. The aim of the investigation was to show whether intermediate complexes may be observed in the oxidation process of $L_2Ru^{(II)}(NCS)_2$ (eq 5) or whether the oxidation proceeds directly to the final dicyanide complex as suggested by Wolfbauer et al.[6]

Experimental Section

Materials. The fully protonated ruthenium complex *cis*-bis(isothiocyanato)bis(2,2′-bipyridyl-4,4′-dicarboxylato)ruthenium(II), $L_2Ru(NCS)_2$, the bis tetrabutylammonium salt of $L_2Ru(NCS)_2$, and *cis*-bis(cyano) (2,2′-bipyridyl-4,4′-dicarboxylato)ruthenium(II), $L_2Ru(CN)_2$, which have the trade names Ruthenium 535, Ruthenium 535-bis TBA, and Ruthenium 505, respectively, were obtained from Solaronix.[9] Dimethylformamide and acetonitrile were HPLC grade (Merc). Lithium trifluoromethansulfonate was purchased from Aldrich.

Instrumentation. The LC-MS instrument was equipped with a UV-diode array detector with a 5-cm flow cell in series with a MS detector. The HPLC instrument was a TSP Spectra system and equipped with an AS3000 auto sampler, P4000 gradient pump, vacuum degasser, and a UV 6000 LP diode array detector. The separation was performed either with gradient program I or II shown in Table 1. The analytical column was a 50 mm Xterra MS RP C18 column from Waters with an i.d. of 2.1 mm. The mass detector was a LCQ-Deca ion trap instrument from ThermoFinnigan equipped with an electrospray ionization interface (ESI) run in positive mode. A positive potential (+4.5 kV) was applied to the silica needle, discharge current 19−20 μA, capillary voltage 23 V, capillary temperature 350 °C, tube lens offset 5 V, sheath gas (N_2), and auxiliary gas (N_2) 78 and 45 arbitrary units, respectively. UV/Vis absorptions were recorded between 400 and 600 nm. The ion trap was run in the data-dependent MS/MS scanning mode. The first scan event was obtained in the *m*/*z* interval 400−800 followed by a second scan event in which an MS^2 spectrum was obtained from either one of the ions selected among the parent mass list or the ion from the first scan event with the highest intensity. Parent mass list: *m*/*z* = 643.1, 648.1, 674.9, 706. Reject mass list: 547, 569, 585, 591, 613, 629, 636, 592. Isolation *m*/*z* width = 6, normalized collision energy 35, activation time 30 ms, and minimum signal required 10^5 counts. The LCQ software Xcalibur 1.2 controlled the chromatographic and mass spectrometric analysis.

Table 1. Applied HPLC Gradient Programs I and II

time/min[a]	A[b] (%)	B[c] (%)
	Gradient I	
0	0	100
5	0	100
18	37	63
23	37	63
36	0	100
41	0	100
	Gradient II	
0	0	100
21.6	100	0
31.6	100	0
36.6	0	100

[a] Eluent flow = 0.2 mL/min. [b] A: Acetonitrile. [c] B: 5% acetonitrile + 94% water + 1% formic acid.

Oxidation of $L_2Ru^{(II)}(NCS)_2$ in DMF. The bis tetrabutylammonium salt of $L_2Ru(NCS)_2$ (30.9 mg, 0.0252 mM) was dissolved in 30 mL of argon deaerated dimethylformamide with 0.02 M $LiCF_3SO_3$ as the supporting electrolyte. The electrolysis was performed at constant potential +1.0 V vs Ag/AgI ($I^- = 0.1$ M) in a three compartment H-cell with a platin electrode as an anode and a carbon rod as a cathode. The electrolysis was followed by withdrawing samples (100 μL) from the anode chamber at regular coulomb intervals and injecting 2 μL of the solution onto the HPLC column. The HPLC analyses were performed with gradient program I (Table 1) and the eluted peaks were detected by UV/Vis and MS.

Oxidation of $L_2Ru^{(II)}(NCS)_2$ in Acetonitrile. The electrolysis of the bis tetrabutylammonium salt of $L_2Ru(NCS)_2$ (14.62 mg, 0.0123 mM) in acetonitrile was performed similarly to the electrolysis in DMF. The HPLC analyses were obtained by the gradient program II (Table 1).

Results and Discussion

Oxidation of $L_2Ru^{(II)}(NCS)_2$ in DMF. A LC-MS chromatogram of the starting complex is shown in Figure 2a. LC-MS and LC-UV chromatograms are shown in Figure 2b and 3a, respectively, of the sample withdrawn from the electrolysis of $L_2Ru(NCS)_2$ in dimethylformamide after consumption of 6.0 coulombs ($n = 2.4$ F/mol). Three main peaks are observed in the total ion chromatogram (TIC) with retention times of 6.3, 12.6, and 16.3 min together with a number of smaller peaks. The MS spectra of the three peaks are shown in Figure 2c−e. The peak eluting at 16.3 min was identified as the starting $L_2Ru(NCS)_2$ complex by the

(7) Kohle, O.; Grätzel, M.; Meyer, A. F.; Meyer, T. B. *Adv. Mater.* **1997**, *9*, 904.
(8) Cecchet, F.; Gioacchini, A. M.; Marcaccio, M.; Paolucci, F.; Roffia, S.; Alebbi, M.; Bignozzi, C. A. *J. Phys. Chem. B* **2002**, *106*, 3926.
(9) Solaronix, www.solaronix.com.

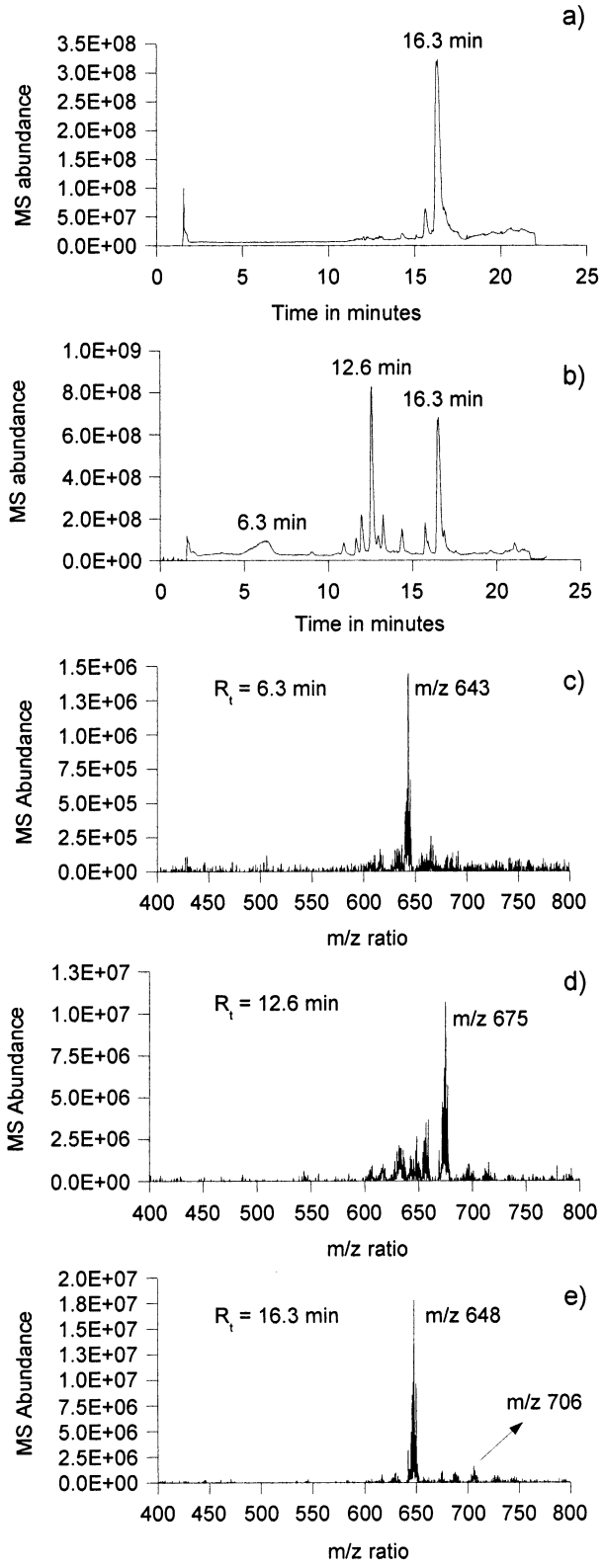

Figure 2. (a) LC-MS total ion chromatogram of the starting complex (0.5 mg/mL) dissolved in dimethylformamide/0.02 M $LiCF_3SO_3$. (b) LC-MS chromatogram of the sample withdrawn from the electrolysis of $L_2Ru(NCS)_2$ after the consumption of 6.0 coulombs (n = 2.4 F/mol). (c) Mass spectra of the $L_2Ru(CN)_2$. (d) Mass spectrum of $L_2Ru(NCS)(CN)$. (e) Mass spectrum of $L_2Ru(NCS)_2$.

Vis spectrum (λ_{max} = 525 nm) and the characteristic ruthenium isotope pattern around the $[L_2Ru^{(III)}(NCS)_2]^+$ ion m/z = 706 shown in Figure 2e. The Vis peak maximum of

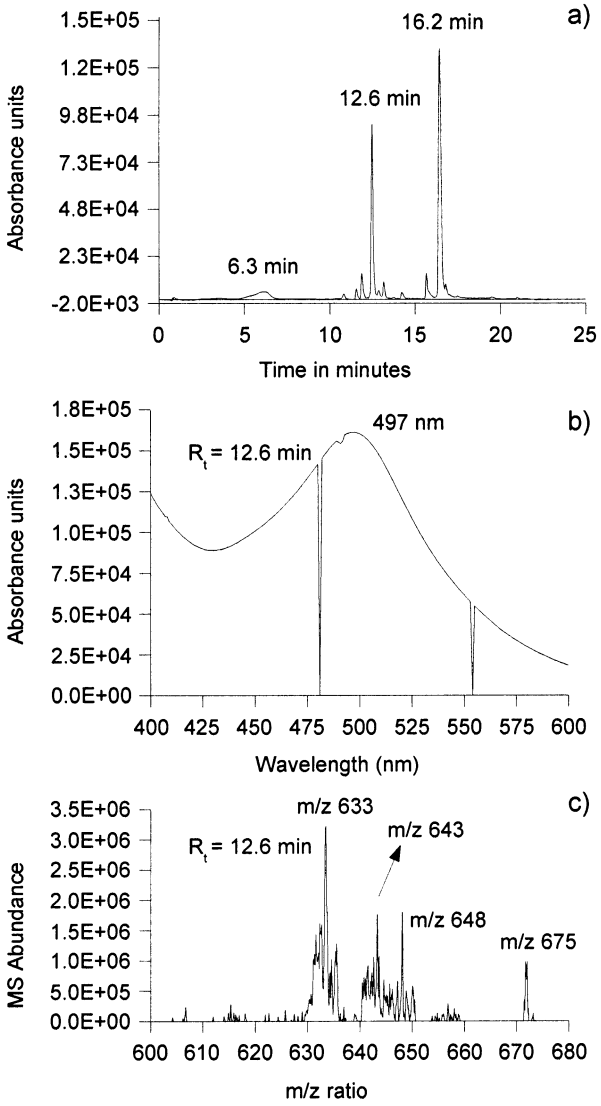

Figure 3. (a) LC-UV chromatogram of the sample withdrawn from the electrolysis of $L_2Ru(NCS)_2$ in dimethylformamide after the consumption of 6.0 coulombs (n = 2.4 F/mol). (b) UV spectrum of $L_2Ru(NCS)(CN)$. (c) MS^2 of the $[L_2Ru(NCS)(CN) + H]^+$ ion m/z = 675.

the L_2RuX_2 complexes have been shown to be solvent-dependent and their peak maxima are shifted to shorter wavelengths in polar solvents.[10] This explains the 13-nm relative blue shift of the $L_2Ru(NCS)_2$ peak in a water/acetonitrile/1% formic acid mixture relative to the 538 nm obtained in pure ethanol.[10] The intensity of the ruthenium isotope pattern around the $[L_2Ru^{(III)}(NCS)_2]^+$ molecular ion m/z = 706 (see Figure 2e) is low due to an easy elimination of one $NCS^\bullet$ radical with the formation of an intense ruthenium isotope distribution pattern around the $[L_2Ru^{(II)}(NCS)]^+$ ion m/z = 648. The broad peak with the retention time 6.3 min has a peak max at λ = 470 nm (shifted 35 nm relative to ethanol) and an intense ruthenium isotope pattern in the mass spectrum (Figure 2c) around the ion m/z = 643, which corresponds to the $[L_2Ru^{(II)}(CN)_2 + H]^+$ ion of the dicyano complex $L_2Ru(CN)_2$. The intense $[L_2Ru^{(II)}(CN)_2 +$

(10) Nazeeruddin, Md. K.; Zakeeruddin, S. M.; Humphry-Baker, R.; Jirousek, M.; Liska, P.; Vlachopoulos, N.; Shklover, V.; Fischer, C.-H.; Grätzel, M. *Inorg. Chem.* **1999**, *38*, 6298.

H]$^+$ ion clearly demonstrates the strength of the Ru−CN bond compared with that of the Ru−NCS bond. The identity of the 6.3-min peak was further verified by injecting an authentic sample of the dicyano complex into the LC-UV-MS instrument. The peak with the retention time 12.6 min is the main intermediate oxidation product. The visible spectrum shown in Figure 3b has a peak maximum at 497 nm and two equal intense ruthenium isotope patterns around $m/z = 675$ in the mass spectrum of the complex (Figure 2d). The $m/z = 675$ may be assigned to the $[L_2Ru^{(II)}(NCS)(CN) + H]^+$ ion of the intermediate complex $L_2Ru(NCS)(CN)$ with the molecular formula $RuC_{26}H_{16}N_6O_8S_1$ and the molecular weight 674 calculated with the most abundant ruthenium isotope ^{102}Ru (21%). The MS^2 spectrum of the $m/z = 675$ is shown in Figure 3c and shows the degradation m/z 675 → 648, 643, and 633 corresponding to the elimination of HCN, S, and CNO, respectively. The retention time of the $L_2Ru(NCS)(CN)$ complex is nearly the average of the retention time of the $L_2Ru(CN)_2$ and $L_2Ru(NCS)_2$ complexes that further substantiates the mixed ligand structure of the intermediate oxidation product. In Figure 4a the total ion chromatogram of the sample withdrawn after 9 C ($n = 3.6$ F/mol) is shown. A large new peak dominates the chromatogram at the retention time 10.9 min with a peak maximum at 493 nm and a ruthenium isotope pattern around $m/z = 689$ (see Figure 4b) corresponding to the solvent complex ion $[L_2Ru^{(II)}(CN)(DMF)]^+$. All the ruthenium complexes, which are eluting from the RP C18 column with retention, are in a neutral form. The complex eluting after 10.9 min is therefore the deprotonated form $[Ru(dcbpyH)(dcbpyH_2)(CN)(DMF)]$. Besides the peaks of the starting complex and the mixed thiocyanate−cyanide complex at 16.3 and 12.6 min, respectively, two smaller peaks are present at 14.3 and 15.8 min, respectively. The latter peak has a Vis maximum at 521 nm and a ruthenium isotope pattern around $m/z = 706$ with a low intensity and an intense ruthenium isotope pattern around $m/z = 648$ (see Figure 4d). The UV/Vis and mass spectra are very similar to the corresponding spectra of the starting complex and may be assigned to the isomer $L_2Ru(NCS)(SCN)$, which is present in small amounts (5%) in the starting complex (see Figure 2a).[10] The low-intensity ruthenium isotope pattern around $m/z = 729$ observed in Figure 4d may be identified as the sodium adduct ion $[L_2Ru^{(II)}(NCS)(SCN) + Na]^+$. The peak at 14.3 min has a UV peak maximum at 493 nm and ruthenium isotope patterns around the m/z values 721 and 648 (see Figure 4c). The $m/z = 721$ corresponds to the ion $[L_2Ru^{(III)}(NCS)(DMF)]^+$ and the $m/z = 648$ is obtained by an elimination of the DMF molecule from the molecular ion, which is further verified by the MS^2 spectrum of $m/z = 721$ (721 → 648).

In Figure 5 the peak areas of the five complexes $L_2Ru(NCS)_2$ ($R_t = 16.3$ min), $L_2Ru(NCS)(CN)$ ($R_t = 12.6$ min), $L_2Ru(NCS)(DMF)^+$ ($R_t = 14.3$ min), $L_2Ru(CN)_2$ ($R_t = 6.3$ min), and $L_2Ru(CN)(DMF)^+$ ($R_t = 10.9$ min) are shown as a function of the amount of charge, which have passed the electrolysis cell. The two DMF complexes are eluted as the neutral compounds $[Ru(dcbpyH)(dcbpyH_2)(NCS)(DMF)]$ and $[Ru(dcbpyH)(dcbpyH_2)(CN)(DMF)]$, respectively. As

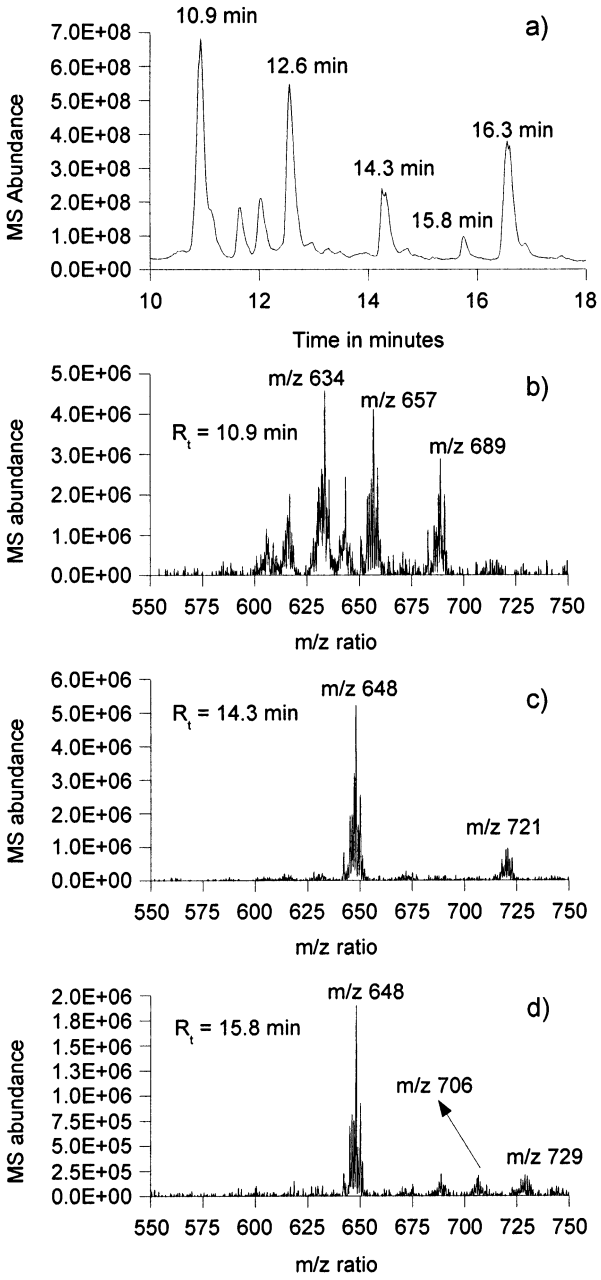

Figure 4. (a) LC-MS chromatogram of the sample withdrawn from the electrolysis of $L_2Ru(NCS)_2$ in dimethylformamide after the consumption of 9.0 coulombs ($n = 3.6$ F/mol). (b) Mass spectrum of $L_2Ru^{(II)}(CN)(DMF)$. (c) Mass spectrum of $L_2Ru^{(II)}(NCS)(DMF)$. (d) Mass spectrum of $L_2Ru(NCS)(SCN)$.

seen from Figure 5, the concentration curves of the two intermediate complexes $L_2Ru(NCS)(CN)$ and $L_2Ru(NCS)(DMF)^+$ and the final oxidation products $L_2Ru(CN)_2$ and $L_2Ru(CN)(DMF)^+$ evolve nearly in the same way. The intermediate complexes obtain their maximal intensity after 9 C ($n = 3.6$ F/mol) and after 10−12 C. $L_2Ru(NCS)_2$, $L_2Ru(NCS)(CN)$, and $L_2Ru(NCS)(DMF)^+$ are oxidized at nearly the same rate, indicating that the oxidation potentials of the three complexes are nearly equal. The oxidation potentials of $L_2Ru(NCS)_2$ and $L_2Ru(CN)_2$ in dimethylformamide have been obtained by cyclic voltammetry to 0.785 and 0.985 V vs SCE, respectively,[6] and the oxidation potential of $L_2Ru(NCS)(CN)$ is likely to be close to the

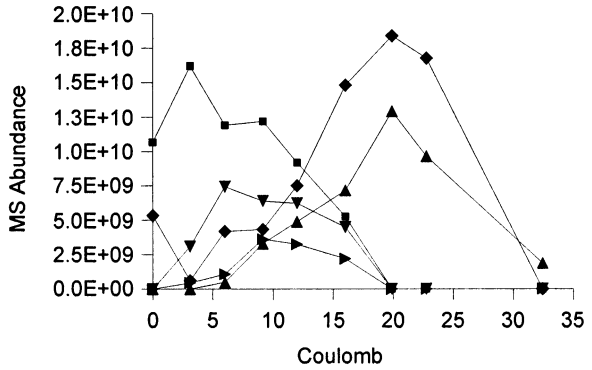

Figure 5. LC-UV areas of the peaks of the five complexes $L_2Ru(NCS)_2$, (■), $L_2Ru(NCS)(CN)$ (▼), $L_2Ru(NCS)(DMF)$ (sideways triangle), $L_2Ru(CN)_2$ (◆), and $L_2Ru(CN)(DMF)$ (▲) as a function of the amount of charge that has passed the electrolysis cell.

average value 0.885 V vs SCE. After 20 C ($n = 8$ F/mol), the $L_2Ru(NCS)_2$ and the two intermediate complexes have disappeared completely and the concentrations of the $L_2Ru(CN)_2$ and $L_2Ru(CN)(DMF)^+$ complexes have obtained their maximum values. The number of electrons transferred during the course of the bulk electrolysis was $n = 8$ per molecule of $L_2Ru(NCS)_2$, which is the same number obtained by Wolfbauer ($n = 6 \pm 2$) within a reasonable degree of uncertainty. When the oxidation potential of the electrolysis was increased to +1.4 V vs SCE, the last two complexes $L_2Ru(CN)_2$ and $L_2Ru(CN)(DMF)^+$ disappeared completely after 33 C. We have unfortunately not been able to identify the final degradation products.

On the basis of the above analysis of the coulometric curves in Figure 5, we suggest that two parallel oxidation routes proceed simultaneously. One mechanism that does not involve the solvent and may occur by an internal oxidation process inside the complex (eq 6) and a mechanism that involves the dimethylformamide solvent (eq 7),

$$L_2Ru(NCS)_2 \rightarrow L_2Ru(NCS)(CN) \rightarrow L_2Ru(CN)_2 \quad (6)$$

$$L_2Ru(NCS)_2 \rightarrow L_2Ru(NCS)(DMF)^+ \rightarrow L_2Ru(CN)(DMF)^+ \quad (7)$$

When dry TiO_2 photo anodes, which have been dyed with $L_2Ru(NCS)_2$, are exposed to light, the red color of the $L_2Ru(NCS)_2$ disappears and a yellow color develops, caused by the formation of the $L_2Ru(CN)_2$ complex.[7] This experiment, which we have checked, demonstrates that a solvent is not needed in the oxidation of $L_2Ru(NCS)_2$ to $L_2Ru(CN)_2$ and supports the idea of two competing routes, a solvent-independent mechanism and a process in which the solvent is involved.

Oxidation of $L_2Ru^{(II)}(NCS)_2$ in Acetonitrile. The LC-MS chromatograms are shown in Figure 6a of a sample withdrawn after 3.0 C ($n = 2.5$ F/mol) from the electrolysis of $L_2Ru(NCS)_2$ in acetonitrile. The chromatograms, which have been obtained by gradient elution program II (Table 1), are dominated by a large peak with $R_t = 6.96$ min (as written in Figure 6a). The peak has a λ_{max} at 482 nm and an intense ruthenium isotope pattern around $m/z = 689$ in the mass spectrum shown in Figure 6b, which may be identified

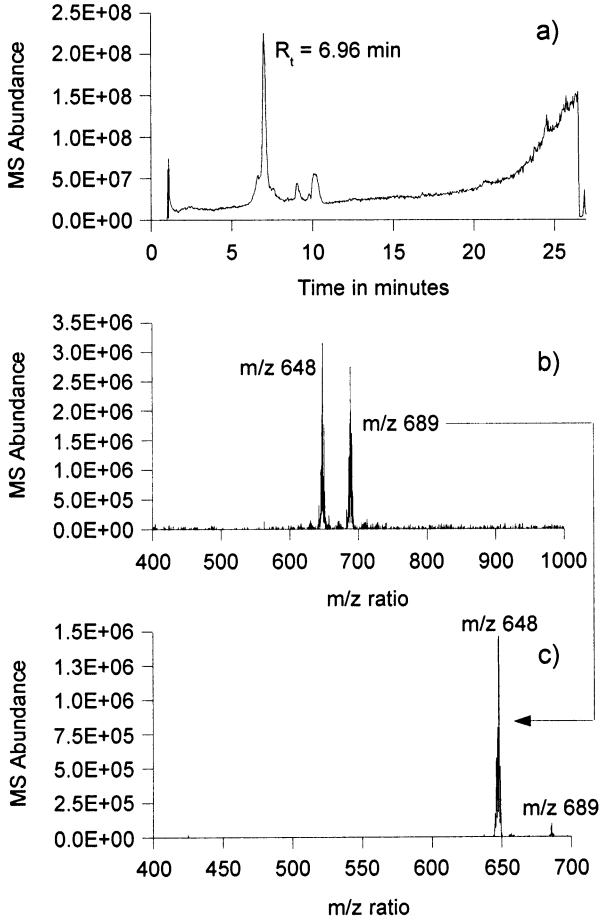

Figure 6. (a) LC-MS chromatogram of the sample withdrawn from the electrolysis of $L_2Ru(NCS)_2$ in acetonitrile after the consumption of 3.0 coulombs ($n = 2.5$ F/mol). (b) Mass spectra of $L_2Ru(NCS)(ACN)$. (c) MS^2 of the $[L_2Ru(NCS)(ACN)]^+$ ion $m/z = 689$.

as the intermediate solvent complex ion $[L_2Ru(NCS)(ACN)]^+$. The structure of the ion may be further substantiated by the MS^2 spectrum of the $m/z = 689$ ion (Figure 6c), which shows the elimination of one acetonitrile molecule m/z 689 → m/z 648. After 9 C ($n = 7.6$ F/mol), this intermediate complex has vanished and a new one appeared at 4.15 min in the LC-UV chromatogram with $\lambda_{max} = 462$ nm and an intense ruthenium pattern around the $m/z = 657$ ion, which may be assigned to the ion $[L_2Ru^{(II)}(CN)(ACN)]^+$ (see Figure 7a−c). After further 3.5 C, the $L_2Ru^{(II)}(CN)(ACN)^+$ complex had disappeared and a new broad peak was detected at $R_t = 3.0$ min with $\lambda_{max} = 449$ nm and ruthenium isotope patterns at $m/z = 821$ (weak) and 739 (intense). We have unfortunately not been able to identify this complex. In all the recorded chromatograms there was no trace of the complexes $L_2Ru(NCS)(CN)$ and $L_2Ru(CN)_2$ as observed in the electrolysis in DMF. Apparently, the internal oxidation mechanism eq 6 appears not to be involved in the oxidation process in acetonitrile. The higher nucleophilicity of the acetonitrile relative to DMF may be the reason a shift in competition between the two mechanisms is observed between ACN and DMF. In acetonitrile the oxidation process follows eq 8:

$$L_2Ru(NCS)_2 \rightarrow L_2Ru(NCS)(ACN)^+ \rightarrow L_2Ru(CN)(ACN)^+ \quad (8)$$

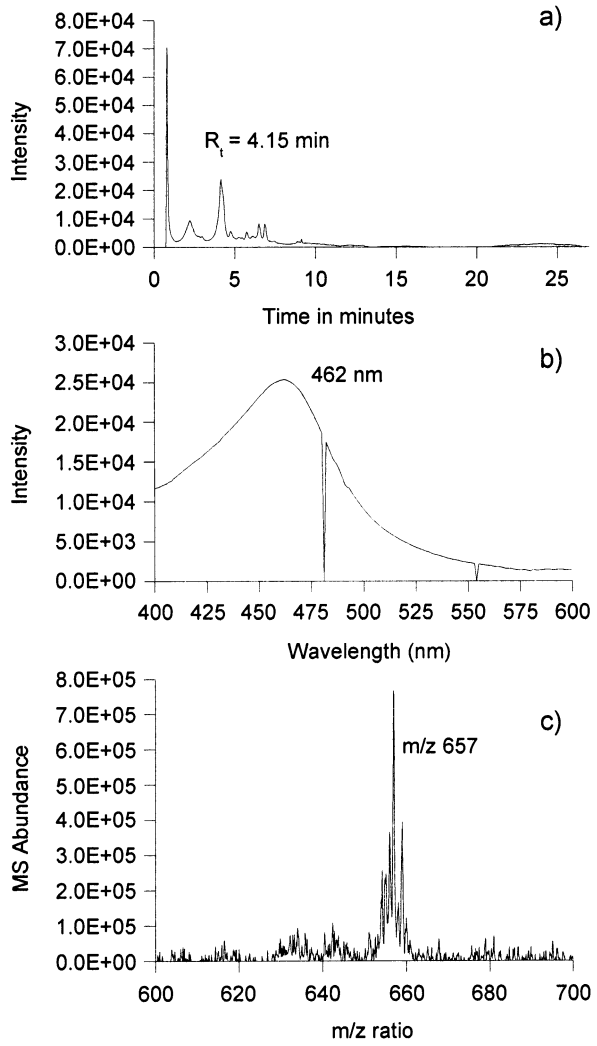

Figure 7. (a) LC-MS chromatogram of the sample withdrawn from the electrolysis of $L_2Ru(NCS)_2$ in acetonitrile after the consumption of 9.0 coulombs (n = 7.6 F/mol). (b) UV spectrum of $[L_2Ru(CN)(ACN)]^+$. (c) MS of the $[L_2Ru(CN)(ACN)]^+$ ion.

The intermediate complex $L_2Ru(NCS)(ACN)^+$ was also observed by Cecchet et al.; however, in their proposed mechanism the final oxidation product was $L_2Ru(ACN)_2^+$, and $L_2Ru(CN)(ACN)^+$ was not observed.[8] While the chromatography of the $L_2Ru(ACN)_2^{2+}$ or the deprotonated form $[Ru^{(II)}(dcbpyH)(dcbpyH_2)(ACN)_2]^+$ is not expected to proceed smoothly on a RP C18 column, we followed the procedure reported by Cecchet et al.[8] and performed a direct infusion ESI-MS analysis of the electrolysis mixture in acetonitrile with tetraethylammonium hexafluorophosphate (0.01 M) as the supporting electrolyte. Because of the ion suppression by the tetraethylammonium ions, we were not able to observe the fragment ion m/z = 630 $[Ru^{(II)}(dcbpyH)(dcbpyH_2)(ACN)]^+$ [8] or any other signals from ruthenium species. $LiCF_3SO_3$ has been reported to be compatible with direct infusion ESI-MS analysis of organic compounds.[11] To our surprise, however, it was not possible to analyze L_2RuX_2 complexes by direct infusion ESI-MS in the presence of $LiCF_3SO_3$. We were therefore not able to confirm the existence of the end electrolyzed product $L_2Ru(ACN)_2^{2+}$.

Conclusion

Four different ruthenium complexes were identified by LC-UV-MS during the electrochemical oxidation process of the solar cell dye $L_2Ru(NCS)_2$ in dimethylformamide. The formation of the four complexes may be explained by a competition between a solvent-independent route (eq 6) with formation of the intermediate complex $L_2Ru(NCS)(CN)$ and the final oxidation product $L_2Ru(CN)_2$ and a solvent-dependent route that proceeds through the intermediate complex $L_2Ru(NCS)(DMF)^+$ to the final product $L_2Ru(CN)(DMF)^+$ (eq 7). In acetonitrile the solvent-dependent mechanism is dominant and only the oxidation products $L_2Ru(NCS)(ACN)^+$ and $L_2Ru(CN)(ACN)^+$ were identified. The solvent-independent process is likely to involve an internal electron transfer between the NCS^- ligand and the ruthenium(III) center as the initial step in the transformation of the starting complex to the intermediate mixed complex $L_2Ru(NCS)(CN)$. The NCS^- ligands are oxidized, one by one, to the cyano ligands as shown in eq 6, and not in a single step as reported previously.[6] In reasonable agreement with the experiments of Wolfbauer et al. we find that an exhaustive electrolysis of $L_2Ru(NCS)_2$ requires the removal of n = 8 electrons per molecule of the starting complex. Furthermore, the work demonstrates the usability of the LC-UV/Vis-MS method for the analysis of L_2RuXY complexes.

Acknowledgment. This work was financially supported by the Danish Energy Authority and Eltra Amba.

IC0207294

(11) Zhou, F.; Berkel, J. V. *Anal. Chem.* **1995**, *67*, 3643.